Absorption spectroscopy of $R^{3+}(R=\mathrm{Pr,Nd})$ ion pairs in $CsCdCl_3$

Samar Jana and Ranajit K. Mukherjee
Department of Solid State Physics, Indian Association for the Cultivation of Science, Calcutta-700032, India
(Received 12 February 1997; revised manuscript received 22 July 1997)

The energy levels of $R^{3+}(R=\mathrm{Pr,Nd})$ ions replacing the divalent Cd^{2+} ions in single crystals of $CsCdCl_3$ have been investigated by polarized absorption at 10 K. For charge balance, a majority of R^{3+} ions in $CsCdCl_3$ form pairs with a vacancy associated with it. The analysis reveals that R^{3+} pair ions are in two unequal sites which result from two arrangements: (i) with a vacancy in between the two R^{3+} ions and (ii) with a vacancy on any one side of the two R^{3+} ions. Indeed two types of spectra are observed due to the different C_{3v} crystal fields at these two sites. Thirteen levels of Pr^{3+}, arising out of five multiplets, and thirty levels of Nd^{3+}, arising out of twelve multiplets, have been identified along with their irreducible representations. The best free-ion and crystal-field parameters for Pr^{3+} have also been determined. [S0163-1829(98)00706-1]

I. INTRODUCTION

The studies[1–6] of the optical and other properties of single crystals of the general formula MDH_3 doped with either trivalent transition metal ions or trivalent rare-earth ions (R^{3+}), where M and D are monovalent and divalent metal ions and H is a halide, respectively, indicate that R^{3+} ions occur in pairs in these crystals. When the MDH_3 types of crystals are doped with trivalent ions, the question of charge balance arises and to maintain charge neutrality three D^{2+} ions are replaced by two trivalent R^{3+} ions. McPherson *et al.*[1] have reported that in $CsMgCl_3$ crystals doped with Cr^{3+} ions, the Cr^{3+} ions have a tendency to aggregate in pairs in unexpectedly large proportions. The electron paramagnetic resonance (EPR) studies[2,3] of Gd^{3+} ions doped in $CsMgCl_3$, $CsMgBr_3$, and $CsCdBr_3$ crystals have demonstrated the existence of Gd^{3+}-Gd^{3+} pairs, when the divalent ion is replaced even by a minimal amount of trivalent rare earth ion, like Gd^{3+}. In comparison to the isolated ions, Gd^{3+} pairs occur more frequently than what could be predicted from simple statistical considerations. This happens because pair formation results in greater stability of the linear chain $CsDH_3$ lattice from the standpoint of charge balance requirements.[2,3] Obviously the pairing up of two trivalent ions and a vacancy permits the accommodation of trivalent ions into a $(DH_3^-)_n$ chain compensating the total charge.[2,3] Using high resolution laser spectroscopy Chaminade *et al.*[4] have shown that in a low concentration Pr^{3+}-doped $CsCdBr_3$ crystal a unique pair line dominates the absorption spectra. Ramaz *et al.*[5] have also arrived at the same conclusion that the majority of the Pr^{3+} ions form pairs in Pr^{3+}:$CsCdBr_3$ crystal. There may be two types of pairs (i) R^{3+}-vacancy-R^{3+} and (ii) vacancy-R^{3+}-R^{3+}. Type (i) should predominate from a symmetry and statistical point of view. However, type (ii) cannot be ruled out at higher concentrations of dopant ions. A selective optical excitation study[6] of Nd^{3+} ions doped in $CsCdBr_3$ shows the existence of these two types of pairs, one, Nd^{3+}-vacancy-Nd^{3+}, another being Nd^{3+}-Nd^{3+}-vacancy, resulting in three types of Nd^{3+} spectra. Different spectra arise because of the differences in the trigonal part of the crystal fields experienced by the Nd^{3+} ions in these two types of arrangements of pairs. It is of interest to find out whether this phenomenon is also present in the case of the rare-earth ions in the host $CsCdCl_3$, because some of these compounds may find an application as laser or luminescent materials. Here we present a detailed study of the optical absorption spectra of the Pr^{3+} and Nd^{3+} ion pairs in $CsCdCl_3$ with varied concentrations.

II. EXPERIMENTAL PROCEDURE

A. Crystal structure and preparation

The crystal structure of MDH_3 types of crystals has been studied thoroughly.[7] Crystals of $CsMgCl_3$,[7] $CsCdBr_3$,[2–5] and $CsCdCl_3$ (Refs. 8 and 9) all have the same space group $P6_3/mmc$ (D_{6h}^4) and the divalent metal ions are in the sites of the point group $3m$ (D_{3d}) symmetry. Furthermore they cleave in a very similar way. The crystal cleavage plane contains the c axis. These facts indicate that all these crystals are isostructural. The octahedral $(DH_6)^{4-}$ units are arranged in infinite arrays forming linear chains of octahedra sharing opposite faces. The chains running parallel to the crystallographic c axis are negatively charged and having an overall stoichiometry $(DH_3^-)_n$, induce a ''quasi-one-dimensional'' character in such compounds.[2–5] The Cs^+ ions balance the charge and occupy positions between chains. When Cd^{2+} is replaced by R^{3+} ($R=\mathrm{Pr,Nd}$), these R^{3+} ions associate in the host in the form of a pair as required for charge balance. Hence the inversion symmetry is destroyed and the point symmetry is reduced at the R^{3+} sites from $3m$ (D_{3d}) to $3m$ (C_{3v}).[4,5,12]

Pure CsCl and $CdCl_2$ in equimolecular proportions and required amounts of RCl_3, for different percentages of R^{3+} are dissolved in HCl and the solution is evaporated to dryness. It is then taken in a quartz ampoule and connected to a diffusion pump. After pumping for two to three days and heating at intervals, the ampoule containing the dehydrated sample is flushed several times with helium gas and then it is sealed, to make sure that the sample is in an inert atmosphere. The quartz ampoule is now lowered down slowly (one centimeter per day) in a lab-made Bridgmann furnace maintained at 565 °C. Good single crystals of R^{3+}:$CsCdCl_3$

nearly 1 cm in length and about 6 mm in diameter are obtained. The 0.5, 1, and 1.5 % Pr^{3+}-doped $CsCdCl_3$ crystals, and 1 and 1.5 % Nd^{3+}-doped $CsCdCl_3$ crystals are studied. These percentages are verified by spectroscopic analysis.

B. Experimental methods

The c axis of the crystal is identified by a polarizing microscope. For optical absorption study, the crystals are carefully cleaved and polished so that the flat planes parallel to the c axis are obtained. The problem of excessive line width and confusing satellite structure in high concentrations of R^{3+}-doped samples is avoided by using thin crystals.[10] Polarized absorption spectra are photographed using a high dispersion plane-grating spectrograph (Carl Zeiss, Jena, PGS2) having a resolution of 0.15 Å in the first order. The crystal is mounted on the tip of a closed-cycle helium cryostat (Air Products) with its c axis in vertical direction. Light from a tungsten halogen lamp is focused on the sample which in turn is focused on the spectrograph slit. In between the crystal and spectrograph a Wollaston prism is placed to polarize the light simultaneously in vertical and horizontal polarizations. The vertically polarized image in which the electric vector of the incident light is parallel to the c axis of the crystal gives $c_{\parallel}$ (i.e., π polarized) and the other in which it is perpendicular to the c axis produces $c_{\perp}$ (i.e., σ polarized) spectra. Thus the spectra in both π and σ polarizations are obtained simultaneously. The wavelengths of the fine absorption lines of R^{3+} are calibrated by a standard mercury lamp. The uncertainty of the observed energies is within $\pm 1\ \mathrm{cm}^{-1}$.

C. Experimental results

1. Pr^{3+}:$CsCdCl_3$ crystals

As observed in the spectra, the optical absorption lines of Pr^{3+} may be grouped mainly in three regions, i.e., 16 680, 20 500, and 22 275 cm^{-1} consisting of several lines in each region. There are two very prominent absorption lines around 21 085 cm^{-1}. The π and σ polarized spectra at different concentrations are indicated in Figs. 1, 2, and 3. These absorption lines correspond to $^3H_4(\Gamma_1)\rightarrow{}^1D_2$, $^3H_4(\Gamma_1)\rightarrow(^3P_0,{}^3P_1,{}^1I_6)$ and $^3H_4(\Gamma_1)\rightarrow{}^3P_2$ transitions, respectively, which compare well with the standard literature[11] and are matched by our own fittings (see Sec. III C below). In all cases, (A) represents π spectra and (B) σ spectra. The energy values of the absorption lines at the highest concentration of 1.5% are given in Table I. However, the transitions observed in 0.5 and 1 % crystals are the same as that of 1.5%, only the intensity of some of the lines is very weak at lower concentrations. Those weak lines are intensified in 1.5% crystal. A separation of 5 to 10 cm^{-1} between the prominent and weak lines is found. Comparison of the spectra of Pr^{3+} with concentrations of 0.5, 1, and 1.5 % as denoted by (a), (b), and (c), respectively, in all the aforesaid figures, shows the following features.

(i) In the σ polarized spectra of the species with lowest Pr^{3+} concentration (0.5%) recorded in the region 16 680 cm^{-1}, three transitions are observed at 16 580, 16 589, and 16 596 cm^{-1} (Fig. 1). At higher concentrations the lines are found to gain intensity, the transitions at 16 589 and 16 596 cm^{-1} being more intense than the one observed at 16 580 cm^{-1}. In the π polarization a rather broad transition at 16 687 cm^{-1} is observed. However, at the lowest concentration this transition is too weak and eludes precise detection. At higher concentration of 1% the line at 16 687 cm^{-1} shows a weak component at 16 693 cm^{-1} and for 1.5% concentration there is practically no change. The σ polarized narrow transition at 17 197 cm^{-1}, on the contrary, is very clear in all the three crystals with different concentrations of Pr^{3+} and exhibits an increase in intensity with concentrations.

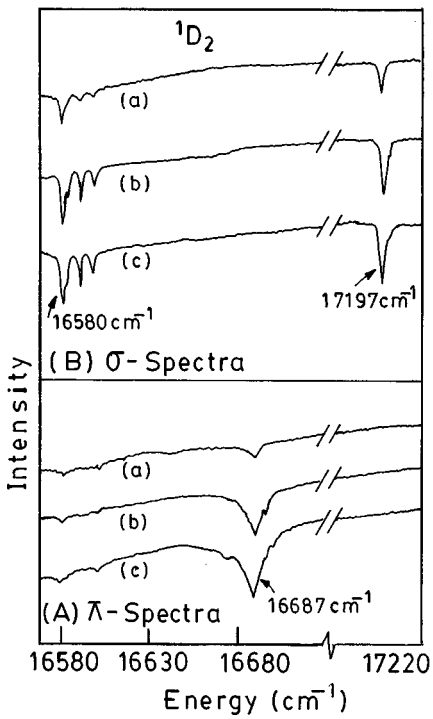

FIG. 1. Polarized absorption spectra for $^3H_4(\Gamma_1)\rightarrow{}^1D_2$ transition observed at 10 K in (A) π polarization and (B) σ polarization. For Figs. 1–3, in both polarizations, (a), (b), and (c) denote 0.5, 1, and 1.5 % concentration of Pr^{3+} doped in $CdCdCl_3$, respectively.

(ii) Around 20 500 cm^{-1} the spectra are very complex (Fig. 2). This region manifests transitions to three multiplets $^3P_0$, $^3P_1$, and $^1I_6$. For the lowest concentration the π transitions at 20 506 and 20 513 cm^{-1} are well resolved, but at higher concentrations these two lines nearly merge with each other and a small dip is seen in the microphotometry trace. Other transitions become intense at a higher concentration of 1.5%. Two π polarized transitions at 21 081 and 21 088 cm^{-1} are observed at all three concentrations.

(iii) Near 22 275 cm^{-1}, a pair of strong π transitions at 22 273 and 22 279 cm^{-1} is recorded and in σ polarization there are two pairs of transitions at 22 190 and 22 327 cm^{-1}. Figure 3 reveals that the nature of these polarized spectra is similar at all concentrations but becomes faint at low concentration. It is noteworthy that the π polarized spectra at 20 506 and 22 273 cm^{-1} exhibit very similar changes with increasing concentrations of Pr^{3+} ions [Figs. 2(A) and 3(A)].

2. Nd^{3+}:$CsCdCl_3$ crystals

At 10 K the polarized absorption lines of Nd^{3+}:$CsCdCl_3$ may be grouped mainly into eight centers, viz., at 16 641,

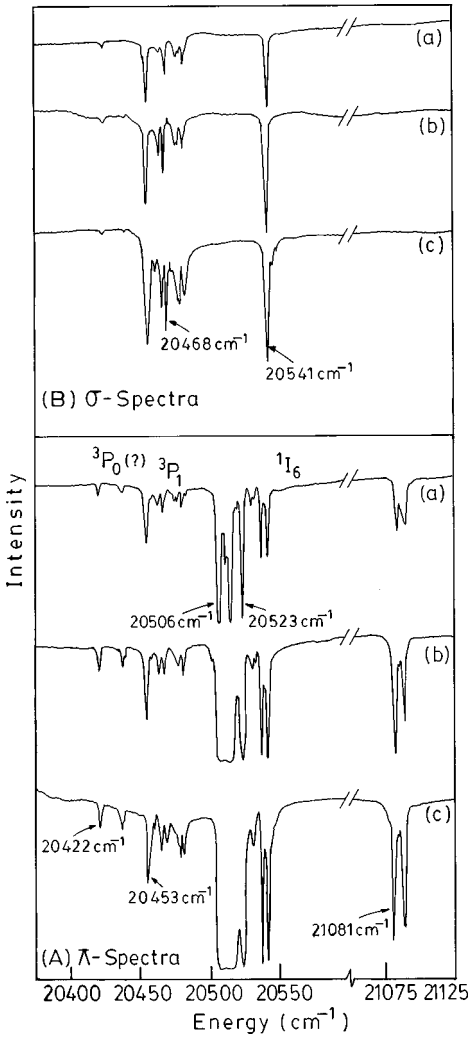

FIG. 2. Absorption spectra of $^3H_4(\Gamma_1) \rightarrow (^3P_0, ^3P_1, ^1I_6)$ multiplets at 10 K, observed in both (A) π and (B) σ polarizations.

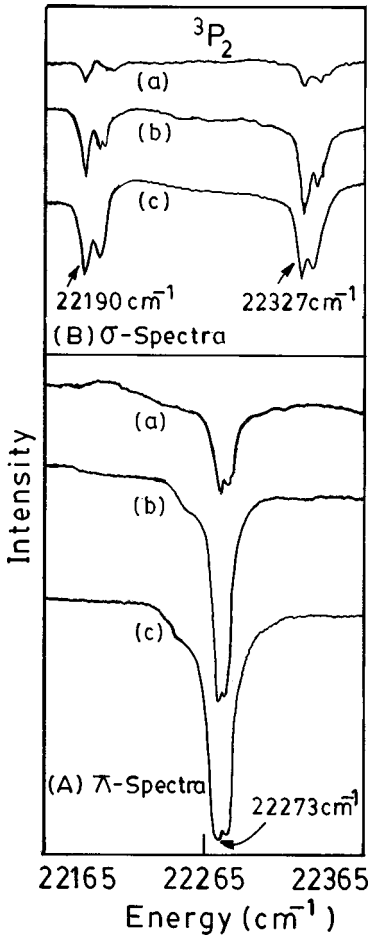

FIG. 3. Experimental absorption spectra of Pr^{3+}-doped $CsCdCl_3$ crystals at various concentrations in both (A) π and (B) σ polarizations at a temperature of 10 K for the $^3H_4(\Gamma_1) \rightarrow {}^3P_2$ transition.

16 878, 17 200, 18 668, 19 209, 20 911, 27 551, and 27 794 cm^{-1}. Reviewing the earlier works on spectra of Nd^{3+}:$CsCdBr_3$,[12] Nd^{3+}:$LaCl_3$,[11,13–15] Nd^{3+} in $LaBr_3$,[16] neodymium ethylsulfate,[11,17] $Cs_2NaNdCl_6$, and Nd^{3+}:Cs_2NaYCl_6 (Ref. 18) crystals, the above energy centers are assigned to $^2H_{11/2}$, $^4G_{5/2}$, $^2G_{7/2}$, $^4G_{7/2}$, ($^4G_{9/2}$,$^2K_{13/2}$), ($^2G_{9/2}$,$^2D_{3/2}$,$^4G_{11/2}$,$^2K_{15/2}$), $^4D_{3/2}$, and $^4D_{5/2}$ multiplets, respectively. The identification of the levels of these multiplets is based on the knowledge of the (Γ_5,Γ_6) nature of the assigned ground state and the fact that level positions do not change much from one compound to another[12] (see Sec. III D and Table II).

In this case also it is found that the spectra vary with concentration. There are some prominent absorption lines at lower concentration (i.e., 1% Nd^{3+}:$CsCdCl_3$) and barring four, each of these lines is accompanied by a weak line at the higher energy side. At higher concentration (i.e., 1.5%) the weak lines become very distinct as observed in Figs. 4, 5, and 6. The two series are separated by 2 to 18 cm^{-1} (the only exception is the level at 17 225 cm^{-1} in the $^2G_{7/2}$ multiplet, where the separation is 32 cm^{-1}). Figures 4, 5, and 6 represent the transitions $^4I_{9/2} \rightarrow {}^2H_{11/2}$, $^4I_{9/2} \rightarrow {}^4G_{5/2}$, and $^4I_{9/2} \rightarrow {}^2G_{7/2}$, respectively. In all these figures (A) indicates π polarized and (B) σ polarized spectra, and (a) and (b) denote results of 1 and 1.5 % Nd^{3+}:$CsCdCl_3$ crystals, respectively. The experimental energy values for the higher concentration are given in Table II. However the energy values for the lower concentration are same, only the intensity of some of the lines is very weak.

III. RESULTS AND DISCUSSION

A. Analysis of spectra

The observed spectra (Figs. 1–6) show that there exist some prominent transitions and each of these transitions is accompanied by a weak transition at the higher energy side of the former one. As the concentration of the dopant is increased, the intensity of the weak lines increases more than that of the prominent lines. The total number of lines in any particular multiplet is more than what would be expected if the R^{3+} (R=Pr,Nd) ion sites have no symmetry (C_1). These extra lines may be due to site effect or due to the distortions of the lattice in the vicinity of the rare-earth ion. However, repeated investigations with the crystals of different batches and of varied concentrations produce the same number of absorption lines in any particular multiplet. Hence the possibility of the effect of lattice distortion is ruled out and the presence of nonequivalent sites is indicated. The large separation (5 to 10 cm^{-1} for Pr^{3+} and 2 to 18 cm^{-1} for Nd^{3+}) between the two series cannot be due to ion-ion ex-

TABLE I. The observed and calculated (using free-ion and crystal-field parameters from Table III) energy values of Pr^{3+} ions in 1.5% Pr^{3+}-doped $CsCdCl_3$ crystal for two different sites along with the assigned C_{3v} irreducible representations. Here ''difference'' is the difference between the observed and calculated energies. All energies are expressed in units of cm^{-1}.

	$\mathcal{A}$ site			$\mathcal{B}$ site			
Multiplet	Obs. energy	Calc. energy	Difference	Obs. energy	Calc. energy	Difference	$[\Gamma_i(\mathcal{A})/\Gamma_i(\mathcal{B})]$
$^3H_4$		0			0		Γ_1
		61			68		Γ_1/Γ_2
		110			117		Γ_3
		185			193		Γ_3
		552			568		Γ_1/Γ_2
		640			648		Γ_3
$^3H_5$		1914			1919		Γ_3
		1942			1946		Γ_1/Γ_2
		1967			1973		Γ_3
		1973			1982		Γ_1/Γ_2
		2332			2343		Γ_3
		2348			2362		Γ_1/Γ_2
		2414			2422		Γ_3
$^3H_6$		3967			3973		Γ_3
		4019			4023		Γ_3
		4047			4058		Γ_1/Γ_2
		4057			4060		Γ_1/Γ_2
		4434			4447		Γ_1/Γ_2
		4470			4482		Γ_3
		4507			4516		Γ_3
		4574			4577		Γ_1/Γ_2
		4583			4585		Γ_1/Γ_2
$^3F_2$		4968			4977		Γ_3
		5062			5073		Γ_3
		5088			5096		Γ_1
$^3F_3$		5438			5450		Γ_1/Γ_2
		5603			5609		Γ_3
		5776			5787		Γ_1/Γ_2
		5817			5822		Γ_3
		6077			6086		Γ_1/Γ_2
$^3F_4$		6083			6095		Γ_3
		6106			6119		Γ_3
		6107			6120		Γ_1/Γ_2
		6202			6211		Γ_1/Γ_2
		6223			6234		Γ_3
		6258			6267		Γ_1/Γ_2
$^1G_4$		8419			8427		Γ_1/Γ_2
		8560			8566		Γ_3
		8651			8660		Γ_1/Γ_2
		8718			8724		Γ_3
		8992			9006		Γ_3
		9056			9065		Γ_1/Γ_2
$^1D_2$	16 580$_{(16\,581)}$	16 586	−6	16 589 (16 596)	16 590	−1	Γ_3
	16 687	16 670	17	16 693	16 678	15	Γ_1
	17 197	17 219	−22		17 232		Γ_3
$^3P_0$?	20 422	20 366	56	20 437	20 375	62	Γ_1

TABLE I. (*Continued*).

	$\mathcal{A}$ site			$\mathcal{B}$ site			
Multiplet	Obs. energy	Calc. energy	Difference	Obs. energy	Calc. energy	Difference	$[\Gamma_i(\mathcal{A})/\Gamma_i(\mathcal{B})]$
$^3P_1$	20 453	20 504	−51	20 463	20 513	−50	Γ_2
	20 468	20 536	−68	$20\,475_{(20\,477)}$	20 545	−70	Γ_3
$^1I_6$	20 506	20 581	−75	20 513	20 585	−72	Γ_1
		20 613			20 616		Γ_3
	20 523	20 628	−105	20 530	20 636	−106	Γ_1
	20 536	20 649	−113	20 541	20 657	−116	Γ_3
		20 760			20 769		Γ_2
	21 081	21 138	−57	21 088	21 149	−61	Γ_1
		21 330			21 346		Γ_2
		21 440			21 453		Γ_3
		21 484			21 498		Γ_3
$^3P_2$	22 190	22 151	39	$22\,200_{(22\,202)}$	22 159	41	Γ_3
	22 273	22 175	98	22 279	22 184	95	Γ_1
	22 327	22 234	93	$22\,335_{(22\,336)}$	22 243	92	Γ_3
$^1S_0$		43 632			43 641		Γ_1

change effect, because the exchange interaction in this case is very small. The analysis[2,3] indicates that the exchange interaction between the two Gd^{3+} paired ions in Gd^{3+}:$CsCdBr_3$, $CsMgBr_3$, and $CsMgCl_3$, is antiferromagnetic but extremely weak, as the ions are far apart and there are no direct superexchange pathways. Hence if the ion-ion exchange interaction is very small, the small splitting of the single ion absorption line due to exchange interaction remains hidden within the linewidth of the observed spectra and the spectra can reasonably be treated as single ion spectra.

As mentioned earlier, due to charge balance the R^{3+} ions occur in pairs in $CsCdCl_3$, and the point symmetry of each R^{3+} ion in the pair becomes C_{3v}. According to Barthou and Barthem,[6] these pairs exist in such a way that the R^{3+} ions experience three different trigonal crystal fields. The arrangements, depicted in Fig. 7, are

(i) Cd^{2+}-$\mathbf{R}^{3+}$-vacancy-$\mathbf{R}^{3+}$-Cd^{2+}, $\mathcal{A}$ type, $\mathcal{A}_1$,$\mathcal{A}_2$ sites;

(ii) Cd^{2+}-R^{3+}-$\mathbf{R}^{3+}$-vacancy-Cd^{2+}, $\mathcal{B}$ type, $\mathcal{B}_1$ site;

(iii) Cd^{2+}-$\mathbf{R}^{3+}$-R^{3+}-vacancy-Cd^{2+}, $\mathcal{B}$ type, $\mathcal{B}_2$ site.

The R^{3+} ion of interest is shown in boldface. In both the $\mathcal{A}_1$,$\mathcal{A}_2$ sites the R^{3+} ion is in between a Cd^{2+} ion and a vacancy. In the $\mathcal{B}_1$ site the R^{3+} ion is in between another R^{3+} and a vacancy, whereas in the $\mathcal{B}_2$ site it is in between a Cd^{2+} ion and a R^{3+} ion. Obviously in the $\mathcal{A}$ type pair both the R^{3+} ions ($\mathcal{A}_1$,$\mathcal{A}_2$) are in equivalent sites but in the $\mathcal{B}$ type the two R^{3+} ions are in two different sites and both $\mathcal{B}_1$ and $\mathcal{B}_2$ sites lack the inversion symmetry. Three different spectra are anticipated from three unequal sites. However, the R^{3+} ions in the $\mathcal{A}_1$,$\mathcal{A}_2$ sites and that in the $\mathcal{B}_1$ site all being near to the vacancy, experience nearly the same trigonal field but the R^{3+} ion in the $\mathcal{B}_2$ site which is away from the vacancy sees a larger trigonal crystal field component.[6] As a result, the spectra originating from R^{3+} ions in the $\mathcal{A}_1$,$\mathcal{A}_2$ sites and the $\mathcal{B}_1$ site are nearly identical. Thus the R^{3+} ions in three unequal sites produce only two different spectra. In our spectra, the series of prominent absorption lines, which occur at all concentrations including the minimal one, originate from a site having larger statistical probability. Such spectra must be due to the $\mathcal{A}_1$, $\mathcal{A}_2$, and $\mathcal{B}_1$ sites. Obviously the other series, whose intensity increases with concentration, must be due to the R^{3+} ions in the $\mathcal{B}_2$ site. The number of ions in the $\mathcal{B}$ type increases with concentration. Because of the similarity of the spectra, to avoid confusion the $\mathcal{A}_1$, $\mathcal{A}_2$, and $\mathcal{B}_1$ sites spectra are designated as $\mathcal{A}$ site spectra and $\mathcal{B}_2$ site spectra, which are the only representatives of the $\mathcal{B}$ type of pair, are called $\mathcal{B}$ site spectra.

B. Selection rules and assignment of levels of Pr^{3+} ions

The selection rules for electric dipole transition under C_{3v} point symmetry are $\Gamma_1 \rightarrow \Gamma_1$ in π, $\Gamma_2 \rightarrow \Gamma_2$ in π, $\Gamma_1 \rightarrow \Gamma_3$ in σ, $\Gamma_2 \rightarrow \Gamma_3$ in σ, and $\Gamma_3 \rightarrow \Gamma_3$ are both in π and σ polarizations, where Γ_1 and Γ_2 are one-dimensional and Γ_3 is a two-dimensional irreducible representation of C_{3v}.[5] The number of transitions and the nature of their polarization in any multiplet are consistent with that of C_{3v} site symmetry and two unequal sites, e.g., the multiplet $^3P_2$ which splits into Γ_1,$2\Gamma_3$ levels under C_{3v} symmetry,[19] shows six components due to two unequal sites ($\mathcal{A}$ site and $\mathcal{B}$ site). The ground multiplet in the $4f^2$ configuration is $^3H_4$, which splits into six levels $2\Gamma_1$,Γ_2,$3\Gamma_3$, for each site, with the lowest being singlet followed by another singlet with a separation of 61 and 68 cm^{-1} for the $\mathcal{A}$ and $\mathcal{B}$ sites, respectively, as found from our calculation. Since the working temperature (10 K) is sufficiently low, transitions occur from either Γ_1 or Γ_2 depending on which one is the ground state and not from both. The polarization study with Γ_1 as the ground state gives the most satisfactory fit with the observed spectra.

It should be mentioned here that the occurrence of an extra σ polarized line at 16 596 cm^{-1} in the $\mathcal{B}$ site of $^1D_2$ multiplet is not clearly understood and the transition at

TABLE II. Observed energy values of 1.5% Nd^{3+}:$CsCdCl_3$ crystal along with the assigned irreducible representations under C_{3v} site symmetry.

	Observed Energy (cm^{-1})		$[\Gamma_i(\mathcal{A})/\Gamma_i(\mathcal{B})]$
Multiplet	$\mathcal{A}$ site	$\mathcal{B}$ site	
$^2H_{11/2}$	16 603		Γ_4
	16 613	16 616	(Γ_5,Γ_6)
	16 618	16 620	Γ_4
	16 642	16 648	Γ_4
	16 667	16 669	Γ_4
	16 675	16 678	(Γ_5,Γ_6)
$^4G_{5/2}$	16 852	16 869	Γ_4
	16 885	16 889	(Γ_5,Γ_6)
	16 900	16 903	Γ_4
$^2G_{7/2}$	17 143	17 161	Γ_4
	17 180	17 185	(Γ_5,Γ_6)
	17 209	17 219	Γ_4
	17 225	17 257	Γ_4
$^4G_{7/2}$	18 566	18 584	Γ_4
	18 643	18 653	Γ_4
	18 716	18 733	Γ_4
	18 760	18 770	(Γ_5,Γ_6)
$(^4G_{9/2},{}^2K_{13/2})$	19 092	19 097	Γ_4
	19 123		Γ_4
	19 148	19 151	(Γ_5,Γ_6)
	19 235	19 241	(Γ_5,Γ_6)
	19 252	19 266	(Γ_5,Γ_6)
	19 320	19 325	(Γ_5,Γ_6)
$(^2G_{9/2},{}^2D_{3/2},$	20 692		(Γ_5,Γ_6)
$^4G_{11/2},{}^2K_{15/2})$	20 817	20 820	(Γ_5,Γ_6)
	20 943	20 949	(Γ_5,Γ_6)
	21 009		(Γ_5,Γ_6)
	21 128	21 130	(Γ_5,Γ_6)
$^4D_{3/2}$	27 547	27 554	(Γ_5,Γ_6)
$^4D_{5/2}$	27 791	27 797	(Γ_5,Γ_6)

20 536 cm^{-1} in the $\mathcal{A}$ site of the $^1I_6$ multiplet does not quite follow the polarization rule. Also the assignment of the $^3P_0$ multiplet is in doubt. As observed in our crystals, the $^3P_0$ multiplet occurs closer to $^3P_1$ compared to what has been found by earlier works.[5,11,18,22] The very weak transitions at 16 581 cm^{-1} in the $\mathcal{A}$ site and at 20 477, 22 202, and 22 336 cm^{-1} in the $\mathcal{B}$ site, that are indicated by the lower suffixes in Table I, may be due to pair ion exchange interaction. These lines are observed in the 1% concentration crystal, whereas at 1.5% concentration the linewidth of these lines increases and they cannot be distinguished from the main line. Also the line broadening and overlapping of some transitions observed in Fig. 2(A) and Fig. 3(A) cannot be explained satisfactorily and may be due to exchange interaction.

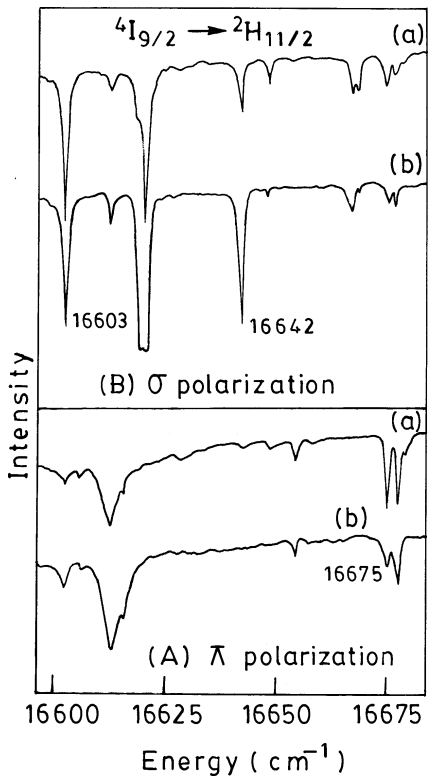

FIG. 4. Absorption spectra of $^4I_{9/2}\rightarrow{}^2H_{11/2}$ transition of Nd^{3+}:$CsCdCl_3$ crystal at various concentrations observed at 10 K in (A) π polarization and (B) σ polarization. In both polarizations, (a) and (b) denote 1 and 1.5 % concentration of Nd^{3+} doped in $CsCdCl_3$, respectively.

C. Free-ion and crystal field parameters fitting for Pr^{3+}

We are interested only in the absorption spectra of Pr^{3+} ions in pairs occupying the two different sites. Since the effect of the exchange interaction is very small, calculation of ion-ion exchange interaction has not been attempted and the total single ion Hamiltonian $H_T=H_f+H_{\mathrm{cf}}$ (free-ion and crystal-field Hamiltonian) is considered as follows:[12]

$$H_f=\sum_{k=0,2,4,6}F^k f_k+\sum_{i=1}^{n}\zeta_{4f}\,l_i\cdot s_i+\alpha L(L+1)+\beta G(G_2)$$
$$+\gamma F(R_7)+\sum_{k=0,2,4}M^k m_k+\sum_{k=2,4,6}P^k p_k, \qquad (1)$$

which includes the usual electrostatic (F^k), spin-orbit (ζ_{4f}), configuration interaction terms (α,β,γ), the spin-spin and spin-other-orbit interactions (M^k), and two-body electrostatically correlated magnetic (spin-orbit) interaction (P^k) terms. The crystal-field Hamiltonian for C_{3v} site symmetry of the Pr^{3+} ion involves six parameters:[12,19]

$$H_{\mathrm{cf}}=B_0^2U_0^2+B_0^4U_0^4+B_3^4(U_{-3}^4-U_3^4)+B_0^6U_0^6$$
$$+B_3^6(U_{-3}^6-U_3^6)+B_6^6(U_{-6}^6+U_6^6), \qquad (2)$$

where B_q^k is the standard (one-electron) crystal field parameter and U_q^k is a one-electron unit tensor operator.

It is well known that the free-ion (FI) parameters vary slightly for different host environments because of crystal-field (CF) effects. In the present case where the host remains

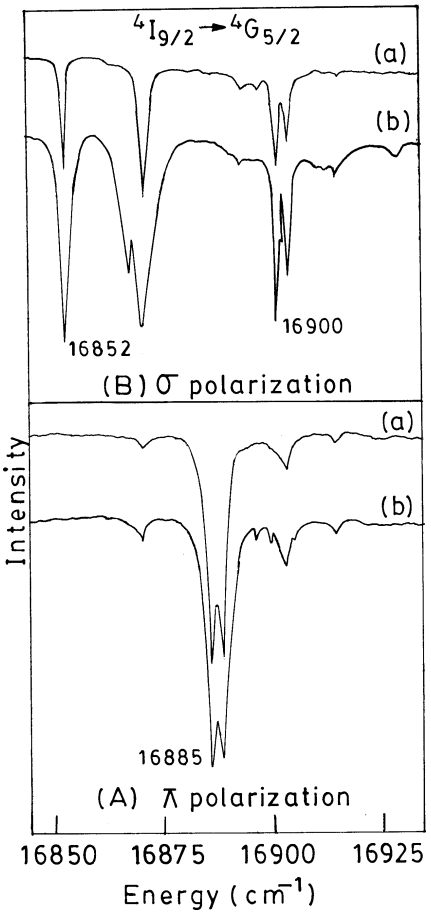

FIG. 5. Observed absorption spectra of the $^4I_{9/2} \rightarrow {}^4G_{5/2}$ transition at 10 K of (a) 1% and (b) 1.5% Nd^{3+}:$CdCdCl_3$ crystals. For Figs. 5 and 6, (A) and (B) denote π and σ polarizations, respectively.

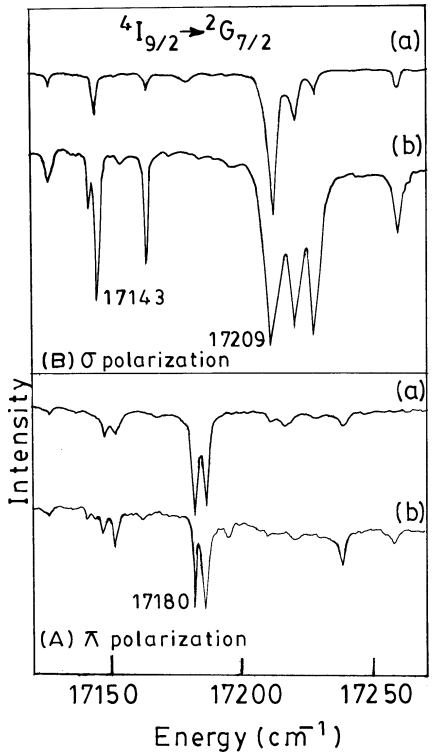

FIG. 6. Experimental absorption spectra of the $^4I_{9/2} \rightarrow {}^2G_{7/2}$ transition at a temperature of 10 K for (a) 1% and (b) 1.5% Nd^{3+}:$CsCdCl_3$ crystals.

the same, there is a small change in the CF between the two different sites. For this, we consider the same FI parameters for the two sites and change only the CF parameters as supported by our experimental findings. In order to fit the complicated spectra due to two types of sites, we have diagonalized the total Hamiltonian (H_T) within the 91 $|\alpha SLJM_J\rangle$ basis sets of the $4f^2$ electronic configuration of the Pr^{3+} ion.

This analysis has been performed using a computer program and minimizing the standard deviation. The program for M^k and P^k has been developed using the definition of Judd *et al.*[20] and the fixed ratios determined from Hartree-Fock calculations for M^k and P^k parameters ($M^2 = 0.56\,M^0$, $M^4 = 0.38\,M^0$ and $P^4 = 0.75\,P^2$, $P^6 = 0.50\,P^2$) are assumed in our analysis.[21]

At first, the $\mathcal{A}$ site energy values are considered for best fitting. Starting with the free-ion parameters for the $Cs_2NaPrCl_6$ system[18,21] the baricenters are optimized using Eq. (1). Then the total Hamiltonian H_T is diagonalized using the standard[19,22] initial trigonal crystal-field parameters. The Slater parameters (F^k) and spin-orbit parameter (ζ_{4f}) are slightly varied and next the crystal-field parameters are varied to obtain a very close match with the observed energy values. Afterwards, all the parameters are varied freely in a single run.[12] In this way the best fitted free-ion and crystal-field parameters are obtained. All the multiplets, including the isolated one ($^1S_0$) at 43 632 cm^{-1}, are identified by recognizing the component with the largest admixture in the eigenfunction. We note that the variations of M^k and P^k parameters with fixed ratios do not produce any remarkable improvement.

For the $\mathcal{B}$ site, which has a different trigonal field, all the six crystal-field parameters are varied to obtain a close match. It is found that all best fitted CF parameters, except B_3^4 and B_3^6, remain unchanged for the $\mathcal{B}$ site.

The theoretical energy values along with their irreducible representations and the observed energy values for highest concentration (1.5% Pr^{3+}:$CsCdCl_3$) are given in Table I. The

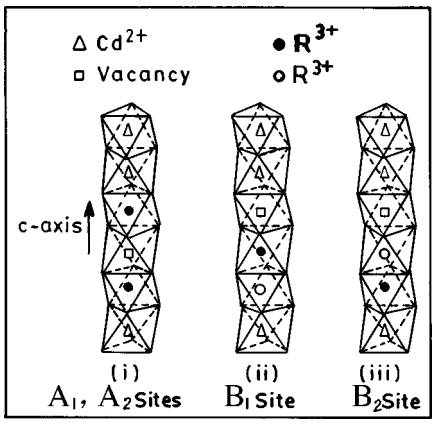

FIG. 7. Arrangements of R^{3+} ions (indicated by dark circles) in pairs in $(CdCl_6)^{4-}$ octahedral chain: (i) equivalent $\mathcal{A}_1, \mathcal{A}_2$ sites: Cd^{2+} vacancy in between the two R^{3+} ions,[5] (ii) $\mathcal{B}_1$ site: R^{3+} ion flanked by a vacancy and another R^{3+}, and (iii) $\mathcal{B}_2$ site: R^{3+} ion in between Cd^{2+} and R^{3+}. The chloride ion occupies the corners of the octahedra.

TABLE III. Free-ion and C_{3v} crystal-field parameters for Pr^{3+} ions in 1.5% Pr^{3+}:$CsCdCl_3$ crystal. Values given in parentheses are held fixed in parameter fitting analysis (Refs. 18 and 21).

Free-ion parameter	Value (cm^{-1})	Crystal field parameter	Value (cm^{-1}) $\mathcal{A}$ site	Value (cm^{-1}) $\mathcal{B}$ site
F^2	69342±21	B_0^2	201±18	201±18
F^4	39374±16	B_0^4	−1453±12	−1453±12
F^6	32267±19	B_3^4	1998±3	2032±4
ζ_{4f}	741±4	B_0^6	−345±16	−345±16
α	25.9±0.12	B_3^6	282±5	236±7
β	(−599)	B_6^6	499±21	499±21
γ	(1520)			
M^0	1.71±0.18			
P^2	(166)			

difference between the observed and calculated energies is designated as ''difference''. The fitted FI and CF parameters for the $\mathcal{A}$ and $\mathcal{B}$ sites are given in Table III. The uncertainty of the CF parameters indicates that if the CF parameters are varied within this range, the calculated energy values do not change significantly.

D. Selection rules and assignment of levels of Nd^{3+} ions

The selection rules for electric dipole transitions, which are dominant for a noncentrosymmetric site, are given in Table IV. Here Γ_4 is a two-dimensional irreducible representation of C_{3v} symmetry, and Γ_5 and Γ_6 are two one-dimensional irreducible representations associated as a Kramer doublet.[12,19]

Since the working temperature (10 K) is low enough, the transitions producing absorption spectra always start from the lowest energy level of the ground multiplet $^4I_{9/2}$, which under the C_{3v} crystal field splits into five levels $2(\Gamma_5,\Gamma_6),3\Gamma_4$ for each site.[19] The lowest level from which the transitions occur will be either (Γ_5,Γ_6) or Γ_4. From the selection rules and the nature of polarization, the possible designation of the ground state has been established by studying the transition of $^4I_{9/2}\rightarrow{}^4G_{5/2}$ (Fig. 5). The multiplet $^4G_{5/2}$ splits into three levels $(\Gamma_5,\Gamma_6),2\Gamma_4$ for each site[19] (i.e., $\mathcal{A}$ and $\mathcal{B}$ site). The existence of the two sites entails a very complicated spectra. In Fig. 5 it is seen that in σ polarization three strong transitions occur at 16 852, 16 869, and 16 900 cm^{-1} and there are two strong π polarized lines at 16 885 and 16 889 cm^{-1}. The transition at 16 903 cm^{-1}, though appears in both the polarizations, is very weak and nearly forbidden in π polarization. If the ground state becomes (Γ_5,Γ_6) then the selection rules suggest that there would be two π polarized and four σ polarized lines for the two sites in the $^4G_{5/2}$ multiplet. On the other hand, if the ground state is Γ_4 then according to the selection rules two σ polarized lines along with the other four lines in both σ and π polarizations are expected to be observed in this transition. Hence the assignment of the ground state is plausibly consistent with the (Γ_5,Γ_6) irreducible representation, as supported also by the number of splitting and the nature of polarization of the transitions $^4I_{9/2}\rightarrow{}^2H_{11/2}$ and $^4I_{9/2}\rightarrow{}^2G_{7/2}$ (Figs. 4 and 6, respectively). The irreducible representations for the levels of the various multiplets are determined in this way.

TABLE IV. Selection rules for electric dipole transition for C_{3v} point symmetry.

C_{3v}	Γ_4	Γ_5	Γ_6
Γ_4	π,σ	σ	σ
Γ_5	σ	π	
Γ_6	σ		π

We note that the σ polarized spectra of $(^2G_{9/2},{}^2D_{3/2},{}^4G_{11/2},{}^2K_{15/2})$, $^4D_{3/2}$, and $^4D_{5/2}$ multiplets are too faint to be recorded properly. The occurrence of the transition at 18 653 cm^{-1} in the $\mathcal{B}$ site of the $^4G_{7/2}$ multiplet in both polarizations is not clearly understood. It may be mentioned that in the transitions to $^2H_{11/2}$, $^4G_{5/2}$, and $^2G_{7/2}$ multiplets a few very weak lines appear in the spectra. These lines may be due to lattice vibrations.

IV. CONCLUSIONS

The R^{3+} ions doped in $CsCdCl_3$ crystal form pairs which are of two types, $\mathcal{A}$ (R^{3+}-vacancy-R^{3+}) and $\mathcal{B}$ (R^{3+}-R^{3+}-vacancy). As the concentration of R^{3+} increases, the intensity of the lines due to the $\mathcal{B}$ site increases, which indicates that the occurrence of the $\mathcal{B}$ type of pair increases too. From the analysis it is clear that the R^{3+} ions see the C_{3v} crystal field in all the sites, whereas the $\mathcal{B}$ sites have a stronger trigonal distortion. From the optical spectra of the $4f^2$ configuration of the Pr^{3+} ions in $CsCdCl_3$, 13 levels with the associated irreducible representations have been determined and the best fit free-ion and crystal-field parameters have been calculated. Similarly from the observed spectra, 30 levels and their irreducible representations of the $4f^3$ configuration of the Nd^{3+} ions in $CsCdCl_3$ have also been determined.

ACKNOWLEDGMENTS

We thank Dr. R. Gupta for providing us some of the computer programs. Also valuable discussions with Professor M. Choudhury, Professor D. Ghosh, and Professor S. P. Ghosh are greatly appreciated.

[1] G. L. McPherson and W. Heung, Solid State Commun. **19**, 53 (1976).

[2] G. L. McPherson and Larry M. Henling, Phys. Rev. B **16**, 1889 (1977).

[3] L. M. Henling and G. L. McPherson, Phys. Rev. B **16**, 4756 (1977).

[4] J. P. Chaminade, R. M. Macfarlane, F. Ramaz, and J. C. Vial, J. Lumin. **48&49**, 531 (1991).

[5] F. Ramaz, R. M. Macfarlane, J. C. Vial, J. P. Chaminade, and F. Madeore, J. Lumin. **55**, 173 (1993).
[6] C. Barthou and R. B. Barthem, J. Lumin. **46**, 9 (1990).
[7] G. L. McPherson, T. J. Kistenmacher, and G. D. Stucky, J. Chem. Phys. **52**, 815 (1970).
[8] Ya. O. Dovgii, I. V. Kityk, S. N. Pidzyrailo, and Z. A. Khapko, J. Appl. Spectrosc. **53**, 1319 (1990).
[9] S. Siegel and E. Gebert, Acta Crystallogr. **17**, 790 (1964).
[10] G. A. Prinz, Phys. Rev. **152**, 474 (1966).
[11] G. H. Dieke, *Spectra and Energy levels of Rare Earth Ions in Crystals* (Wiley, New York, 1968).
[12] R. B. Barthem, R. Buisson, and R. L. Cone, J. Chem. Phys. **91**, 627 (1989).
[13] E. H. Carlson and G. H. Dieke, J. Chem. Phys. **29**, 229 (1958).
[14] E. H. Carlson and G. H. Dieke, J. Chem. Phys. **34**, 1602 (1961).
[15] F. Varsanyi and G. H. Dieke, J. Chem. Phys. **36**, 835 (1962).
[16] I. Richman and E. Y. Wong, J. Chem. Phys. **37**, 2270 (1962).
[17] J. B. Gruber and R. A. Satten, J. Chem. Phys. **39**, 1455 (1963).
[18] F. S. Richardson, Michael F. Reid, John J. Dallara, and Robert D. Smith, J. Chem. Phys. **83**, 3813 (1985).
[19] B. G. Wybourne, *Spectroscopic Properties of Rare Earths* (Interscience, New York, 1965).
[20] B. R. Judd, H. M. Crosswhite, and H. Crosswhite, Phys. Rev. **169**, 130 (1968).
[21] H. M. Crosswhite and H. Crosswhite, J. Opt. Soc. Am. B **1**, 246 (1984).
[22] S. Hufner, *Optical Spectra of Transparent Rare Earth Compounds* (Academic, New York, 1978).